ELSEVIER

Biophysical Chemistry 111 (2004) 205–212

Biophysical Chemistry

www.elsevier.com/locate/bpc

Effects of a hairpin polyamide on DNA melting: comparison with distamycin and Hoechst 33258

Peter L. James[a], Loic Le Strat[a], Ulf Ellervik[b], Christina Bratwall[c], Bengt Nordén[c], Tom Brown[d], Keith R. Fox[a,*]

[a] *Division of Biochemistry and Molecular Biology, School of Biological Sciences, University of Southampton, Bassett Crescent East, Southampton SO16 7PX, UK*

[b] *Organic and Bioorganic Chemistry, Centre for Chemistry and Chemical Engineering Lund University, Box 124, SE 221 00 Lund, Sweden*

[c] *Department of Physical Chemistry, Chalmers University of Technology, SE-412 96 Göteborg, Sweden*

[d] *School of Chemistry, University of Southampton, Highfield, Southampton SO17 1BJ, UK*

Received 2 February 2004; received in revised form 1 June 2004; accepted 1 June 2004
Available online 2 July 2004

Abstract

We have used DNase I footprinting and fluorescence melting studies to study the interaction of the hairpin polyamide Im-Py-Py-Py-$(R)_{H_2N}$γ-Im-Py-Py-Py-β-Dp with its preferred binding sites (5′-WGWWCW; W = A or T) and other sequences. DNase I footprinting confirmed that the ligand binds to the sequence AGAACA at nanomolar concentrations and that changing the terminal A to G causes a dramatic decrease in affinity, while there was no interaction with the reverse sequence WCWWGW. Fluorescence melting studies with 11-mer duplexes showed that the polyamide had very different effects on the forward (TGWWCT) and reverse (TCTAGT) sequences. At low concentrations, the polyamide produced biphasic melting curves with TGATCT, TGTACT and TGAACT, suggesting a strong interaction. In contrast, the melting profiles with TCTAGT were always monophasic and showed much smaller concentration dependent changes in T_m. The polyamide also showed weak binding to the sequence TGATCT when one of the central AT pairs was replaced with an AC mismatch. These melting profiles were compared with those produced by the AT-selective minor groove binding agents distamycin and Hoechst 33258 at the same sites and at similar sequences containing A_5 and $(AT)_3$, which are expected to bind distamycin in the 1:1 and 2:1 modes, respectively. These ligands produced simple monophasic melting curves in which the T_m steadily increased as the ligand concentration was raised.

Keywords: Polyamide; Distamycin; Hoechst 33258; Molecular beacons; DNA melting

1. Introduction

Sequence specific recognition of the DNA minor groove has been achieved by hairpin polyamides that contain pyrrole (Py) and imidazole (Im) residues [1–4]. These ligands are based on the natural compounds distamycin (Fig. 1b) and netropsin which bind to tracts of four or more consecutive A/T base pairs. These were first shown to bind as monomers in the minor groove [5], though it was later shown that distamycin can bind to some sequences as an antiparallel side-by-side dimer [6]. The 1:1 complex is favoured at A_n targets, due to their narrow minor groove, while the 2:1 complex is favoured at regions of alternating AT.

The synthetic polyamides exploit this 2:1 binding mode and recognize specific sequences by the side-by-side pairing of aromatic amino acids in the minor groove. Pyrrole opposite imidazole (Py/Im) targets a C.G base pair whereas Im/Py targets G.C. The Py/Py pair binds both A.T and T.A base pairs [7–11]. The correct pairings are promoted by joining the two halves of the dimer, using a 2,4-diaminobutyric acid linker and the C-terminus usually contains a β-alanine and a (3-dimethylaminopropyl)amino group. Both of these groups facilitate recognition of AT residues [7]. Polyamides bind to DNA with very high affinity, and dissociation constants in the nanomolar range have been

* Corresponding author. Tel.: +44-23-8059-4374; fax: +44-23-8059-4459.
E-mail address: K.R.Fox@soton.ac.uk (K.R. Fox).

0301-4622/$ - see front matter © 2004 Elsevier B.V. All rights reserved.
doi:10.1016/j.bpc.2004.06.001

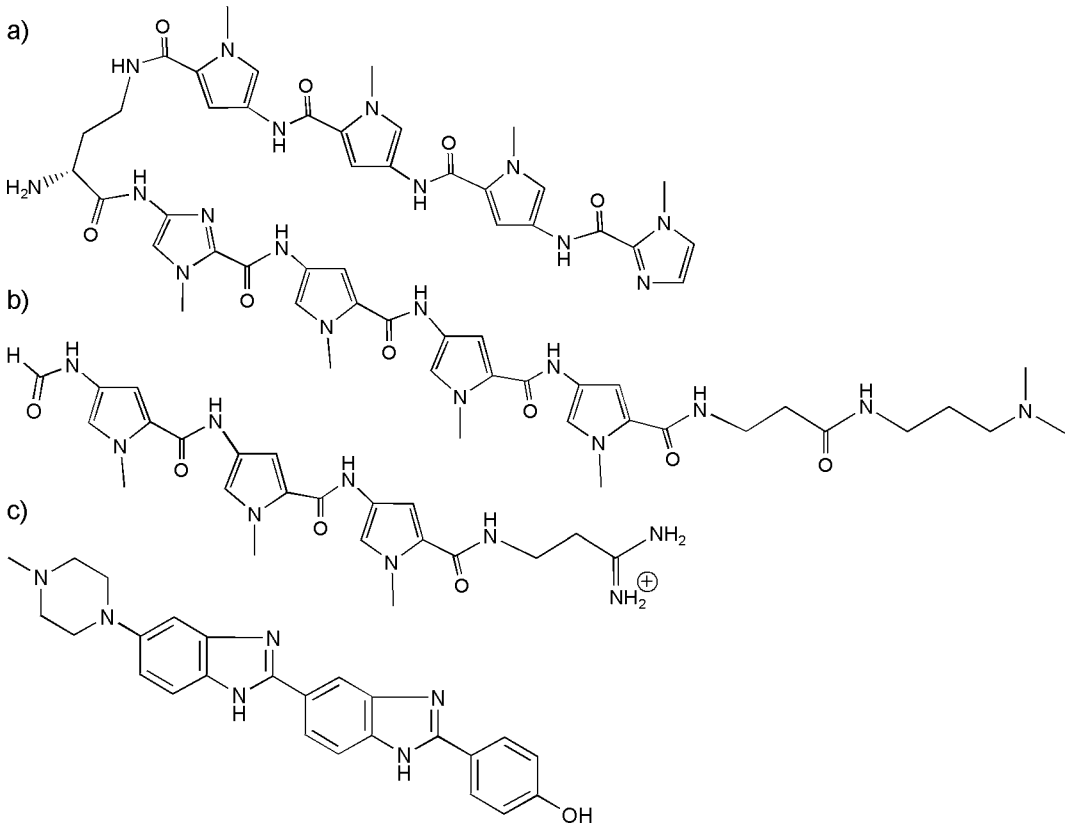

Fig. 1. Structures of (a) Im-Py-Py-Py-(R)$_{H_2N}$γ-Im-Py-Py-Py-β-Dp, (b) distamycin and (c) Hoechst 33258.

reported [12,13]. This high affinity allows them to compete with DNA binding proteins and polyamides have been shown to inhibit the binding of transcription factors NF-kB, TF111A, Est-1, LEF-1 and TBP [14–16].

We have recently developed a novel fluorescence technique for measuring the thermal melting of DNA duplexes [17]. This uses synthetic oligonucleotides that contain a fluorophore and quencher, which are in close proximity in duplex DNA, thereby quenching the fluorescence. When the duplex melts, the fluorophore and quencher are separated and there is a large increase in fluorescence. We have used this technique to study the interaction of the hairpin polyamide Im-Py-Py-Py-(R)$_{H_2N}$γ-Im-Py-Py-Py-β-Dp (Fig. 1a) [13,18] with 11-mer duplexes that contain its cognate target sites 5′WGWWCW3′ (W = A or T). The preferred binding sites were also confirmed by DNase I footprinting. The melting curves were compared with the effects of distamycin and Hoechst 33258 (Fig. 1b,c) on sequences containing the targets AAAAA and ATATAT.

2. Experimental section

2.1. Oligonucleotides

Oligonucleotides were made on the 0.2 μmol scale by standard solid-phase methods using 2-cyanoethyl di-isopropylaminophosphoramidites. The quencher-containing oligonucleotides were synthesised using a 3′-thymidine synthesis column then adding either methyl red serinol phosphoramidite or pyrenebutyryl L-threoninol phosphoramidite. The full synthesis of the pyrene monomer will be presented elsewhere. All 5′-Fluorescein oligonucleotides were synthesised using 6-FAM phosphoramidite (isobutyryl-protected fluoresceinamidohexyl amidite, Cruachem). All oligonucleotides were purified by reversed-phase HPLC. The sequences of these intermolecular duplexes, which contain polyamide and distamycin binding sites, are shown in Fig. 2. For the polyamide targets, 11-mer sequences were chosen so as to generate duplexes with different arrangements of the central bases in the expected WGWWCW target site, generating the sites TGATCT, TGTACT and TGAACT. A fourth target contained this site in the reverse orientation (TCTAGT). A fifth duplex was also prepared in which one of the central AT pairs in TGATCT was replaced with an AC mismatch. The particular GC-rich flanking sequences were chosen so as to reduce the likelihood of misannealing. The fluorophore was always located next to the same base (C) so as to minimise any differences in fluorescence emission.

2.2. Ligands

The polyamide Im-Py-Py-Py-(R)$_{H_2N}$γ-Im-Py-Py-Py-β-Dp [13,18] was synthesised from 0.6 mmol/g Boc-β-

Sequence	Name
Polyamide targets	
5′-F-CCG**TGATCT**GC 3′-Q-GGC**ACTAGA**CG	TGATCT
5′-F-CCG**TGTACT**GC 3′-Q-GGC**ACATGA**CG	TGTACT
5′-F-CCG**TGAACT**GC 3′-Q-GGC**ACTTGA**CG	TGAACT
5′-F-CCG**TCTAGT**GC 3′-Q-GGC**AGATCA**CG	TCTAGT
5′-F-CCG**TGATCT**GC 3′-Q-GGC**ACCAGA**CG	AC mismatch
Distamycin targets	
5′-F-CGC**AAAAA**GGC 3′-Q-GCG**TTTTT**CCG	1:1 TARGET
5′-F-CGC**ATATAT**GGC 3′-Q-GCG**TATATA**CCG	2:1 TARGET

Fig. 2. Sequences of the intermolecular duplexes used in this work. Fluorescein (F) and pyrene (Q) were incorporated at the 5′- and 3′-ends of the two duplex strands, respectively. The polyamide and distamycin binding sites are shown in bold.

PAM-resin by solid phase methods [19,20]. Its concentration was determined by measuring the absorbance at 310 nm with a Hitachi U-2000 spectrophotometer, using a molar extinction coefficient of 69520 M^{-1} cm^{-1}. Distamycin and Hoechst 33258 were purchased from Sigma.

2.3. Fluorescence melting curves of intermolecular duplexes

Fluorescence melting profiles were determined using a Roche LightCycler as previously described [17]. The principle of this technique is that the fluorophore and quencher are in close proximity when a duplex is formed, and the fluorescence is quenched. On denaturing the complex, the fluorophore and quencher are separated and there is a large increase in fluorescence. This technique has several advantages over conventional UV-melting analysis; it requires lower concentrations and smaller volumes, has a high throughput (32 samples in parallel), and it is not affected by any absorbance from the ligand at 260 nm. Duplexes were prepared in 10 mM sodium phosphate pH 7.4 containing 200 mM NaCl. Each sample (20 μl) contained 0.25 μM duplex DNA and 0–40 μM polyamide. The complexes were denatured by heating to 95 °C at a rate of 0.1 °C s^{-1} and maintained at this temperature for 5 min before cooling to 30 °C at 0.1 °C s^{-1}. Samples were then held at 30 °C for 5 min before melting again by heating to 95 °C at 0.1 °C s^{-1}. The fluorescence was recorded during both melting and annealing phases. The LightCycler excites the samples at 488 nm, and the emission was measured at 520 nm. T_m values, indicating the mid-point of the transition at this oligonucleotide concentration, were determined from the first derivatives of the melting profiles using the Roche LightCycler software and were reproducible to within 0.5 °C. Unless otherwise stated, the T_m values quoted refer to the second melting profile. For these complexes there was little or no hysteresis between the melting and annealing curves, indicating that the system is at thermodynamic equilibrium during the temperature changes.

2.4. DNase I footprinting

The footprinting substrate was prepared by cloning the oligonucleotide sequence 5′-GATCCGTTCTCGCTGTTC-TACGCTCTTGTCGCACTTGC into the *Bam*HI site of pUC18. A radiolabelled DNA fragment containing this sequence was prepared by digesting the plasmid with *Hin*dIII and *Sac*I and was labelled at the 3′-end of the *Hin*dIII site using reverse transcriptase and α-^{32}P-dATP. This fragment contains the correct binding site for the polyamide (AGAACA) together with a site with one base difference (AGAACG) and two sites in the reverse orientation (ACAAGA and GCAAGT); these sites are separated by the sequence CGC. The isolated DNA was dissolved in 10 mM Tris–HCl pH 7.5 containing 0.1 mM EDTA to give about 10–20 c.p.s. per μl as determined on a hand held Geiger counter (< 10 nM). For quantitative footprinting experiments, the absolute DNA concentration is not important, so long as it is lower than the dissociation constant of the DNA binding compound [21], since formation of the complexes is limited by the dissociation constant of the reaction and not the stoichiometric ratio of ligand to DNA

For footprinting experiments radiolabelled DNA (1.5 μl) was mixed with 1.5 μl polyamide (dissolved in 10 mM Tris–HCl, containing 10 mM NaCl) to give a final ligand concentration of 5 nM–500 μM, and the mixture was left to equilibrate for at least 2 h. The samples were digested by adding 2 μl DNase I (typically 0.01 Units ml^{-1}) dissolved in 20 mM NaCl containing 2 mM $MgCl_2$ and 2 mM $MnCl_2$. The reaction was stopped after 1 min by adding 5 μl of 80% formamide containing 10 mM EDTA, 10 mM NaOH and 0.1% (w/v) bromophenol blue. The products of digestion were separated on 9% polyacrylamide gels containing 8 M urea. Samples were heated to 100 °C for 3 min, before rapidly cooling on ice and loading onto the gel. Polyacrylamide gels (40 cm long, 0.3 mm thick) were run at 1500 V for about 2 h and then fixed in 10% (v/v) acetic acid. These were transferred to Whatmann 3MM paper and dried under vacuum at 80 °C. The dried gels were either exposed to autoradiography at − 70 °C using an intensifying screen, or were subjected to phosphorimaging using a Molecular Dynamics STORM phosphorimager.

The intensity of bands within each footprint was estimated using ImageQuant software. These were normalised by comparison with a region for which DNase I cleavage was not affected. Footprinting plots [21] were constructed from these data and C_{50} values, indicating the ligand concentration which reduces the band intensity by 50%, were calculated by fitting a simple binding curve to the data.

3. Results

3.1. DNase I footprinting

We first confirmed the preferred binding sequence for this polyamide by DNase I footprinting. According to the rules for pairing of imidazole and pyrrole, the predicted binding site for this ligand is WGWWCW. A footprinting fragment was therefore designed containing one version of this target (AGAACA), together with three other related sequences. The results of these experiments are shown in Fig. 3. A clear footprint can be seen at the expected target site, which persists to nanomolar concentrations. Quantitative analysis of the footprint yielded a C_{50} value of 16 ± 7 nM. The site with a single base change at the 3′-end (AGAACG) is protected from cleavage only at the highest ligand concentrations (850 nM), demonstrating the selectivity of the binding reaction. Cleavage at the reverse sequence (ACAAGA) is only slightly attenuated at highest concentration, while the reverse target with one base modification (GCAAGT) shows no protection.

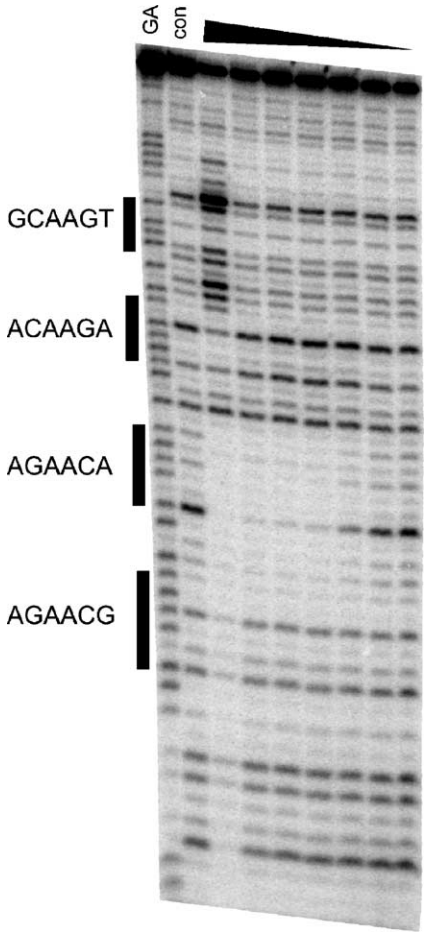

Fig. 3. DNase I footprinting pattern produced by polyamide Im-Py-Py-Py-$(R)_{H_2N}$γ-Im-Py-Py-Py-β-Dp. The potential binding sites are indicated by the filled boxes. The track labelled GA is a marker specific for purines. Con indicates control cleavage in the absence of added ligand. The other lanes show the cleavage pattern in the presence of the polyamide at concentrations of 850, 430, 140, 67, 30, 10 and 5 nM.

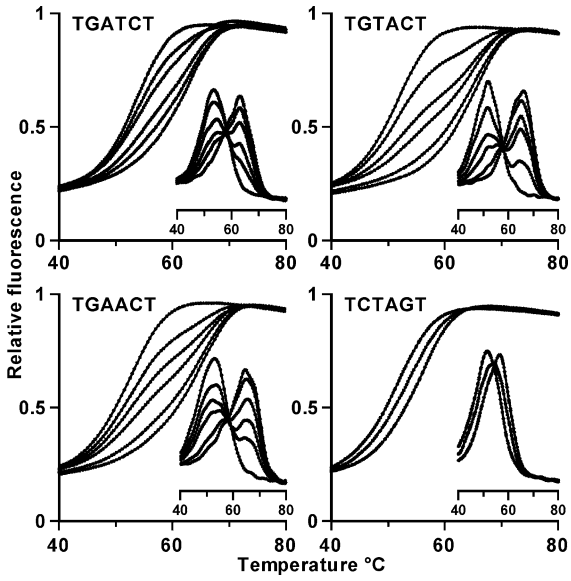

Fig. 4. Fluorescence melting curves for intermolecular duplexes in the presence of different concentrations of the polyamide. The sequences of the duplexes are shown in Fig. 2. The experiments were performed in 10 mM sodium phosphate pH 7.4, containing 200 mM NaCl and 0.25 μM duplex DNA. The inserts show the first derivatives of the melting profiles. The ordinate shows the relative fluorescence of the samples, which has been normalised to the same final value. The abscissa shows the temperature in °C. For TGATCT, TGTACT and TGAACT the curves correspond to polyamide concentrations of 0, 0.2, 0.4, 0.6, 0.8 and 1.0 μM, increasing from left to right. For TCTAGT the concentrations were 0, 0.4 and 1.0 μM.

3.2. Fluorescence melting studies

We have previously shown that fluorescently labelled oligonucleotides can be used for determining the thermal stability of DNA duplexes using a Roche LightCycler [17]. These experiments use fluorescently labelled oligonucleotides in which the fluorophore and quencher are in close proximity in the duplex, and fluorescence is quenched. When the duplex melts, the fluorophore and quencher are separated and there is a large increase in the fluorescence signal. Fig. 4 presents the fluorescence melting experiments for four 11-mer duplexes in the presence of varying concentration of the polyamide. Three of these sequences contain good binding sites for this polyamide (TGATCT, TGTACT, TGAACT) while the fourth contains the reverse

sequence (TCTAGT). In the absence of polyamide, these duplexes melt at similar temperatures with T_m values of 53.7, 51.9, 52.9 and 51.5 °C, respectively. On adding the polyamide, there are clear changes in the melting profiles of the sequences that contain the correct binding sites. At ligand concentrations below 1 μM, these melting curves are biphasic and show two melting transitions, which are more clearly seen in the first derivative plots shown in the inset to each panel. A new melting transition appears at around 65 °C, the proportion of which increases with increasing ligand concentration. A single transition corresponding to the ligand–DNA complex is observed at concentrations above 1 μM. This effect is different to the melting profiles seen with most DNA binding ligands (see below) in which the melting curves progressively shift to higher temperatures on adding more ligand. The two transitions that we observe presumably correspond to the uncomplexed duplex DNA, which melts at the original T_m, and a DNA–polyamide complex with a T_m of around 65 °C. On addition of higher concentrations of the polyamide (2–40 μM), the single melting transition shifted to progressively higher temperatures (not shown). This is presumably due to much weaker (nonspecific) binding, and is similar to the profiles seen with other sequences (see below). These melting experiments cannot be used to determine minor differences between the three good binding sites, but it can be seen that each one produces the same biphasic melting pattern in the presence of the polyamide. Similar results were obtained when the rate of temperature change was decreased from 0.1 °C s^{-1} to 0.5 °C min^{-1}, and there was no significant difference between the melting and annealing curves. Increasing the incubation of the complex before the first melt also had no effect on the melting profiles.

The polyamide has a very different effect on the sequence containing the reverse binding site TCTAGT (Fig. 4, fourth panel). In this case, the changes are more typical of those seen for other small molecule–DNA interactions. With this sequence, there is a single melting transition at all polyamide concentrations, which shifts to higher temperatures with increased ligand concentrations. The polyamide concentration that produced a half-maximal change in T_m of the 0.25 μM duplex was 1.8 ± 0.3 μM. This suggests that the interaction of the polyamide with the reverse sequence is weaker and is in much faster dynamic equilibrium.

The experiments described above used a covalently attached pyrene moiety as the quenching agent, whereas our previous studies [17] employed methyl red. We therefore ensured that the unusual melting profiles did not result from addition of the fluorophore or quencher. Fluorescence melting experiments with similar oligonucleotides containing methyl red instead of pyrene gave similar shaped profiles in the presence and absence of the polyamide (data not shown). The only difference was that the T_m values of duplexes containing pyrene quenchers were about 3 °C higher than those with methyl red quenchers. It therefore appears that the pyrene quencher has a small effect on stabilizing the DNA duplexes. We also performed experiments with similar oligonucleotides that did not contain a quencher. In this case, there was a much smaller change in the fluorescence signal on melting the duplex, but the profiles retained the same shapes, with T_ms that were about 4 °C lower. Positioning the fluorophore and quencher at opposite ends of the duplex also produced melting profiles with a small fluorescence change with T_m values that were increased by about 1 °C. Experiments with these different oligonucleotides show that the fluorophore and quencher have some small effect on the duplex stability, but this does not affect the shapes of the profiles or the interaction with the polyamide ligand.

3.3. Binding to an AC mismatch

Sequence specific recognition by polyamides is largely due to the two-amino group of guanine, which forms a hydrogen bond with the imidazole ring, but generates an unfavourable steric clash with a pyrrole ring. We therefore investigated whether a Py/Py pair can also bind to an AC mismatch, using a duplex in which the central T in the lower strand is replaced by a C (Fig. 2). The results are shown in Fig. 5. It can be seen that introducing this AC mismatch lowered the T_m by 16 °C, compared to the same duplex with

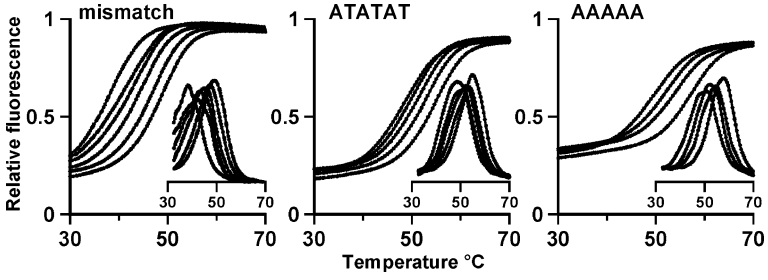

Fig. 5. Fluorescence melting curves for intermolecular duplexes in the presence of different concentrations of the polyamide. The sequences of the duplexes are shown in Fig. 2. The experiments were performed in 10 mM sodium phosphate pH 7.4, containing 200 mM NaCl and 0.25 μM duplex DNA. The inserts show the first derivatives of the melting profiles. The ordinate shows the relative fluorescence of the samples, which has been normalised to the same final value. The abscissa shows the temperature in °C. For mismatch, the curves correspond to polyamide concentrations of 0, 0.6, 1.0, 2, 10 and 20 μM, increasing from left to right. For ATATAT, the polyamide concentrations were 0, 2, 5, 10 and 20 μM, while for AAAAA the concentrations were 0, 2, 5 and 20 μM.

an AT base pair. Addition of the polyamide to this mismatch-containing duplex produced monophasic melting curves, in which the T_m steadily increased with increasing polyamide concentration, with a half-maximal change in T_m produced with 1.8 ± 0.6 μM ligand. The effect on this duplex is similar to that seen with the reverse target site, and indicates weaker binding.

3.4. Interaction with distamycin and Hoechst 33258

We used similar fluorescence melting experiments to study the interaction of distamycin and Hoechst 33258 (Fig. 1b,c) with their AT-rich binding sites. The two duplexes used for these studies are shown in Fig. 2. One contained the central sequence AAAAA, to which distamycin should bind in a 1:1 mode, while the other contained the central sequence ATATAT, to which it should bind in the 2:1 mode. Hoechst 33258 binds to all AT-target sites in the 1:1 mode. Fluorescence melting curves for both ligands with these sequences are shown in Fig. 6. It can be seen that as expected, both ligands increase the melting temperature of both duplexes, and produce monophasic melting curves at all ligand concentrations. The T_m values are listed in Table 1 over a wide range of ligand concentrations. Plotting the ΔT_m values against ligand concentration reveals that in each case, there is a steep rise in melting temperature at low micromolar concentrations, which presumably corresponds to sequence specific binding. This is followed by a slow increase in T_m at higher concentrations (>100 μM), representing secondary, nonspecific binding. In each case, the ligands produce monophasic melting curves at all ligand concentrations, suggesting that they bind less strongly than the hairpin polyamide. There is little difference between the behaviour of the sites designed for 1:1 and 2:1 binding by distamycin.

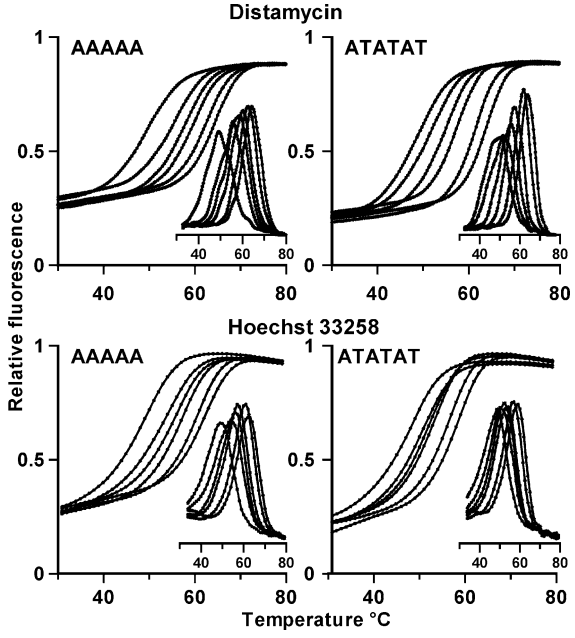

Fig. 6. Fluorescence melting curves for the AT-containing intermolecular duplexes in the presence of different concentrations of distamycin and Hoechst 33258. The experiments were performed in 10 mM sodium phosphate pH 7.4, containing 200 mM NaCl and 0.25 μM duplex DNA. The inserts show the first derivatives of the melting profiles. The ordinate shows the relative fluorescence of the samples, which has been normalised to the same final value. The abscissa shows the temperature in °C. The curves correspond to polyamide concentrations of 0, 0.5, 1.0, 2, 5 and 10 μM, increasing from left to right.

Table 1
Effects of distamycin, Hoechst 33258 and Im-Py-Py-Py-$(R)_{H_2N}$γ-Im-Py-Py-Py-β-Dp on the melting temperatures of different AT-containing duplexes

Concentration (μM)	Distamycin		Hoechst 33258		Polyamide	
	1:1 target	2:1 target	1:1 target	2:1 target	1:1 target	2:1 target
0	49.3	49.8	49.6	48.9	49.9	48.4
0.25	54.7	50.8	52.2	49.6		
0.5	55.5	51.7	54.3	50.6		
1	58.5	55.7	56.2	52.2	51.3	49.4
2	60.2	57.3	57.2	53.7	52.6	51.0
5	62.5	61.7	60.9	56.5	54.0	52.2
10	64.3	63.7	62.4	58.8	55.5	53.2
20	67.7	66.8	63.8	60.2	58.1	55.0
50	70.0	69.3	65.3	62.9	59.5	57.4
100	71.5	71.8	70.3	70.4		
200	73.5	73.7	78.7	78.1		

The fluorescence melting experiments were performed in 10 mM sodium phosphate pH 7.4, containing 200 mM NaCl and 0.25 μM duplex DNA. Melting temperatures (T_m) are in °C.

We also tested the effects of the hairpin polyamide on these AT-rich sites. Representative melting curves for these are shown in Fig. 5, while the T_m values are presented in Table 1. It can be seen that the hairpin polyamide produces a steady increase in the melting temperature of these duplexes at concentrations well above 1 μM. This is very different to the results with the duplexes that contained its best binding site. Although the polyamide can bind to these distamycin sites, it clearly has a lower affinity.

Table 2 shows the effects of distamycin and Hoechst 33258 on melting of the polyamide target sites. From these it can be seen that the T_m values increase on addition of large concentrations of the ligands (much higher than are required to produce changes with the AT-rich binding sites). Plotting these ΔT_m values against ligand concentration produces simple hyperbolic curves with C_{50} values (the ligand concentration causing a half-maximal change in T_m) of between 20 and 40 μM for distamycin and around 300 μM for Hoechst 33258.

4. Discussion

This present study has demonstrated that the fluorescence-melting technique [17] can be used for examining the interaction of minor groove-binding ligands with duplex DNA. These studies have confirmed that the hairpin poly-

Table 2
Effects of Hoechst 33258 and distamycin on melting of the duplexes containing the polyamide binding sites

Concentration (μM)	Hoechst 33258				Distamycin			
	TGATCT	TGTACT	TGAACT	TCTAGT	TGATCT	TGTACT	TGAACT	TCTAGT
0	53.5	51.4	51.5	51.5	53.8	51.9	53.2	53.3
2	53.5	51.2	52.0	51.8	54.7	52.8	54.0	53.7
5	54.0	51.9	53.8	52.0	57.0	55.0	55.3	54.8
10	56.1	53.5	54.5	53.0	59.4	58.1	57.9	57.8
20	57.4	54.1	56.0	53.9	62.0	60.2	61.1	59.7
50	61.5	60.0	59.9	59.1	64.2	63.7	63.2	62.9
100	68.6	66.5	69.4	66.0	66.5	65.3	66.3	64.2
200	76.7	75.1	76.7	74.0	69.0	67.5	67.6	67.5

The fluorescence melting experiments were performed in 10 mM sodium phosphate pH 7.4, containing 200 mM NaCl and 0.25 μM duplex DNA. Melting temperatures (T_m) are in °C.

amide Im-Py-Py-Py-(R)$_{H_2N}$γ-Im-Py-Py-Py-β-Dp binds tightly to its duplex target WGWWCW. Melting studies of this ligand with its cognate sequences produced unusual biphasic melting curves, which indicate strong interaction between the ligand and its target sequence. There have been surprisingly few reports of UV-melting studies with the polyamides, but inspection of the published data also shows biphasic curves [22,23]. There are a number of possible explanations for the biphasic nature of DNA melting curves. McGhee [24] noted that biphasic melting curves can be produced with polynucleotides by one of three possible mechanisms: (1) large tightly binding ligands which are free to transfer between sites, (2) irreversible binding in which ligands cannot transfer between free and bound states and (3) cooperative interaction between ligands. Clearly, the third option is not possible with these synthetic fragments as each one only contains a single ligand binding site, precluding any possibility of cooperativity. Although the ligand–DNA interaction is not irreversible, the biphasic curves can be explained by suggesting that the ligand is in very slow exchange with the free DNA, effectively producing two non-interconverting species, free and bound DNA, which melt at different temperatures. The proportion of the bound species will increase with increasing ligand concentrations. However, biphasic transitions have previously been noted for the interaction of ligands with polynucleotides [24–26], and are explained by suggesting that as the complexes begin to melt, the concentration of free ligand increases, thereby further stabilizing the remaining duplex regions. In either case, it is clear that the biphasic melting curves are indicative of strong binding. Biphasic curves are not observed when distamycin and Hoechst 33258 interact with their preferred AT-rich binding sites, instead the monophasic melting curves shift to progressively higher temperatures as the ligand concentration is increased. This suggests that these molecules bind less tightly in both the 1:1 and 2:1 modes, even though binding constants of 10^7 M^{-1} and greater have been reported for distamycin [28,29].

These data reveal that the polyamide binds much less well to the reverse sequence WCWWGW. A recent combinatorial approach, determining the preferred binding sites for these ligands from a mixed population of oligonucleotides, revealed significant interaction with some reverse sequences [27]. The data presented in this paper show that, although this interaction is stronger than that with non-cognate sites, it is much weaker than to the forward sites. Monophasic melting curves, with a steady increase in T_m with increasing ligand concentrations, are observed with the reverse target site, suggesting that this complex is much weaker.

These results show that the hairpin polyamide binds much less well when an AC mismatch is placed within its binding site instead of an AT base pair. The monophasic melting curves with this sequence show that the hairpin polyamide binds with a similar affinity as to the reverse binding site. Sequence specific binding of polyamides is largely determined by the formation of hydrogen bonds between their imidazole groups and the two-amino groups of guanines. Indeed, polyamides have been used to recognize both GT and GG mismatches [30]. This weaker binding to an AT-mismatch, which is nonetheless stronger than to nonspecific sites, demonstrates that ligand binding must be influenced by the local DNA structure.

Acknowledgements

This work was supported by a grant from the European Union. The LightCycler was partly funded by the BBSRC (JREI).

References

[1] D.E. Wemmer, Designed sequence-specific minor groove ligands, Annu. Rev. Biophys. Biomol. Struct. 29 (2000) 439–461.
[2] P.B. Dervan, Molecular recognition of DNA by small molecules, Bioorg. Med. Chem. 9 (2001) 2215–2235.
[3] P.B. Dervan, R.W. Burli, Sequence-specific DNA recognition by polyamides, Curr. Opin. Chem. Biol. 3 (1999) 688–693.
[4] D.E. Wemmer, P.B. Dervan, Targeting the minor groove of DNA, Curr. Opin. Struct. Biol. 7 (1997) 355–361.

[5] M.L. Kopka, C. Yoon, D. Goodsell, P. Pjura, R.E. Dickerson, The molecular-origin of DNA drug specificity in netropsin and distamycin, Proc. Natl. Acad. Sci. U. S. A. 82 (1985) 1376–1380.
[6] J.G. Pelton, D.E. Wemmer, Structural characterization of a 2-1 distamycin A.d(CGCAAATTGGC) complex by two-dimensional NMR, Proc. Natl. Acad. Sci. U. S. A. 86 (1989) 5723–5727.
[7] C.L. Kielkopt, E.E. Baird, P.B. Dervan, D.C. Rees, Structural basis for G.C recognition in the DNA minor groove, Nat. Struct. Biol. 5 (1998) 104–109.
[8] W.S. Wade, M. Mrksich, P.B. Dervan, Design of peptides that bind in the minor groove of DNA at 5′-(A,T)G(A,T)C(A,T)-3′ sequences by a dimeric side-by-side motif, J. Am. Chem. Soc. 114 (1992) 8783–8794.
[9] M. Mrksich, W.S. Wade, T.J. Dwyer, B.H. Geierstanger, D.E. Wemmer, P.B. Dervan, Antiparallel side-by-side dimeric motif for sequence-specific recognition in the minor groove of DNA by the designed peptide 1-methylimidazole-2-carboxamide netropsin, Proc. Natl. Acad. Sci. U. S. A. 89 (1992) 7568–7590.
[10] S. White, E.E. Baird, P.B. Dervan, On the pairing rules for recognition in the minor groove of DNA by pyrrole–imidazole polyamides, Chem. Biol. 4 (1997) 569–578.
[11] M. Mrksich, M.E. Parks, P.B. Dervan, Hairpin peptide motif—a new class of oligopeptides for sequence-specific recognition in the minor-groove of double-helical DNA, J. Am. Chem. Soc. 116 (1994) 7983–7988.
[12] J.M. Turner, S.E. Swalley, E.E. Baird, P.B. Dervan, Aliphatic/aromatic amino acid pairings for polyamide recognition in the minor groove of DNA, Chem. Soc. 120 (1998) 6219–6226.
[13] J.W. Trauger, E.E. Baird, P.B. Dervan, Recognition of DNA by designed ligands at subnanomolar concentrations, Nature 382 (1996) 559–561.
[14] N.R. Wurtz, J.L. Pomerantz, D. Baltimore, P.B. Dervan, Inhibition of DNA binding by NF-kappa B with pyrrole–imidazole polyamides, Biochemistry 41 (2002) 7604–7609.
[15] L.A. Dickinson, R.J. Gulizia, J.W. Trauger, E.E. Baird, D.E. Mosier, J.M. Gottesfeld, P.B. Dervan, Inhibition of RNA polymerase II transcription in human cells by synthetic DNA-binding ligands, Proc. Natl. Acad. Sci. U. S. A. 95 (1998) 12890–12895.
[16] J.M. Gottesfeld, L. Neely, J.W. Trauger, E.E. Baird, P.B. Dervan, Regulation of gene expression by small molecules, Nature 387 (1997) 202–205.
[17] R.A.J. Darby, M. Sollogoub, C. McKeen, L. Brown, A. Risitano, N. Brown, C. Barton, T. Brown, K.R. Fox, High throughput measurement of duplex, triplex and quadruplex melting curves using molecular beacons and a LightCycler, Nucleic Acids Res. 30 (2002) e39.
[18] C.C.C. Wang, U. Ellervick, P.B. Dervan, Expanding the recognition of the minor groove of DNA by incorporation of beta-alanine in hairpin polyamides, Bioorg. Med. Chem. 9 (2001) 653–657.
[19] E.E. Baird, P.B. Dervan, Solid phase synthesis of polyamides containing imidazole and pyrrole amino acids, J. Am. Chem. Soc. 118 (1996) 6141–6146.
[20] D.M. Herman, E.E. Baird, P.B. Dervan, Stereochemical control of the DNA binding affinity, sequence specificity, and orientation preference of chiral hairpin polyamides in the minor groove, J. Am. Chem. Soc. 120 (1998) 1382–1391.
[21] J.C. Dabrowiak, J. Goodisman, in: N.R. Kallenbach (Ed.), Chemistry and Physics of DNA–ligand Interactions, Adenine Press, New York, 1989, pp. 143–174.
[22] D.S. Pilch, N. Poklar, A.A. Gelfand, S.M. Law, K.J. Breslauer, E.E. Baird, P.B. Dervan, Binding of a hairpin polyamide in the minor groove of DNA: sequence-specific enthalpic discrimination, Proc. Natl. Acad. Sci. U. S. A. 93 (1996) 8306–8311.
[23] D.S. Pilch, N. Poklar, E.E. Baird, P.B. Dervan, K.J. Breslauer, The thermodynamics of polyamide-DNA recognition: hairpin polyamide binding in the minor groove of duplex DNA, Biochemistry 38 (1999) 2143–2151.
[24] J.D. McGhee, Theoretical calculations of the helix-coil transition of DNA in the presence of large cooperatively binding ligands, Biopolymers 15 (1976) 1345–1375.
[25] D.M. Crothers, Statistical thermodynamics of nucleic acids melting transitions with coupled binding equilibria, Biopolymers 10 (1971) 2147–2460.
[26] C.H. Spink, S.E. Wellman, Thermal denaturation as tool to study DNA–ligand interactions, Methods Enzymol. 340 (2001) 193–211.
[27] Y.N.V. Gopal, M.W. Van Dyke, Combinatorial determination of sequence specificity for nanomolar DNA-binding hairpin polyamides, Biochemistry 42 (2003) 6891–6903.
[28] R. Baliga, D.M. Crothers, On the kinetics of distamycin binding to its target sites on duplex DNA, Proc. Natl. Acad. Sci. U. S. A. 97 (2000) 7814–7818.
[29] D. Rentzeperis, L.A. Marky, T.J. Dwyer, B.H. Geierstanger, J.G. Pelton, D.E. Wemmer, Interaction of minor-groove ligands to an AAATT/AATTT site-correlation of thermodynamic characterization and solution structure, Biochemistry 34 (1995) 2937–2945.
[30] E.T. Lacy, E.M. Madsen, M. Lee, W.D. Wilson, in: M. Demeunynck, C. Bailly, W.D. Wilson (Eds.), RNA and DNA binders, vol. 2, Wiley-VCH, Weimnheim, 2002, pp. 384–413.